Temporal Variations of the Statistical Properties of an Underwater Acoustic Channel Measured at a Shallow Water in 2009

Sea-Moon Kim, Sung-Hoon Byun, Seung-Geun Kim, and Yong-Kon Lim
Ocean System Engineering Research Dept., MOERI / KORDI
104 Sinseong-ro, Yuseong-gu
Daejeon 305-343, Korea

***Abstract*-Complicated and time-varying environment of the ocean makes it difficult to describe properties of underwater acoustic channels. Therefore, many researchers have tried to characterize underwater channels using a statistical approach. Although theoretical analysis shows that the probability density function (PDF) of the propagation channel may have Rayleigh or Rician distribution, we still do not know how the statistical properties change for different time and conditions. Recently, Kim et al. and Borowski confirmed again experimentally that PDFs can be fitted to Rayleigh or Rician distributions. However, the results are based on limited data of very short time. In this paper the change of statistical properties are examined using long time observation. Not only magnitude and phase but also phase change rate is analyzed. The results show that the statistical parameters are changing continuously with a certain amount.**

I. Introduction

An Underwater acoustic channel is characterized as time-varying and multipath environment. As acoustic waves from a transmitter propagate through the ocean, they are reflected by the sea surface and bottom which causes a multipath channel to a receiver. Moreover, the inhomogeneous medium scatters the waves and generates numerous micro-paths to the receiver. Because the sea surface and the medium are moving continuously, the channel impulse response is changing and hard to be estimated. In the point of underwater acoustic communication this makes us to consider various ocean conditions for the development of underwater acoustic modems. It is no wonder for that the more we know about transmission channels the better we can design acoustic modems. Therefore, we need to gather channel data as much as possible and analyze them precisely. Many researchers have studied on underwater acoustic propagation channel models for various applications [1-4]. However the results for indentifying communication channels is limited to special cases, for example, a low frequency range.

In order to identify a shallow water acoustic channel around 25kHz, MOERI/KORDI has measured impulse responses near the southern coast of South Korea in November 2007. Kim et al. have shown that the channel responses are highly dependent on frequency and distance, which are also related to angular profile of incident waves [5-6]. In the experiment directional transducers were used.

This work is supported by Ministry of Land, Transport and Maritime Affairs (Project Code #: PMS2020, Development of Underwater Acoustic Network System)

In August 2008, at the same site, MOERI/KORDI has performed a sea-trial to measure impulse responses of the shallow-water acoustic channel [7]. Not only pure tone signals were transmitted but also broadband signals were used to characterize each propagation path. The results showed that the magnitude and phase of the channel response through surface reflected path fluctuate with more severe extent compared to the direct and bottom reflected paths. The authors also found that the probability density function (PDF) of the magnitude for each path has its own characteristics whereas the PDFs obtained from the pure tone signals can be fitted as Rayleigh or Rician distributions. However, we should note that the results are obtained from very limited length of data (120s for each data set). Because the ocean environment changes throughout a day we need to examine how the propagation channel varies during a long period of time.

In November 2009, another field experiment was performed. Its main purpose was to observe the temporal fluctuations of a propagation channel for longer time. As in the experiment in 2008, both narrowband and broadband signals were used for channel probing: one pure tone signal (25kHz) and three broadband signals. In this paper pure tone data are analyzed and their temporal variation is discussed based on the estimated parameters of fitted curves.

In chapter II the experimental method is described briefly. In the next chapter PDFs are obtained and statistical parameters are estimated. The results for different data sets are compared and discussed.

II. Description of the Experiment

The measurement of underwater acoustic channel data has been done at Jinhae Bay near the southern coast of Korea, in November, 2009. An omni-directional projector (ITC-1001) was used for sound transmission and an omni-directional hydrophone (B&K Type 8103) was used for receiving signals. The transducers were deployed from two moored surface vessels and the distance between them was about 120m. The water depth at the measurement site was around 10m. The

978-1-4244-5222-4/10/$26.00 ©2010 IEEE

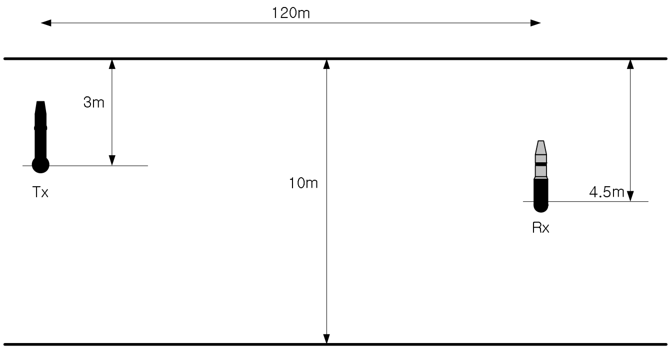

Figure 1. Measurement configuration.

depths of the transmitting and receiving transducers were 3m and 4.5m respectively (see Figure 1).

Pure tone sound of 25kHz was transmitted and 7 received data samples were gathered with the interval of 30 minutes. The length of each sample was 300s and the sampling frequency was 200kHz. Just before the each measurement 30s hydrophone data were recorded to obtain background noise (see Figure 2). We also measured wind speed with intervals of less than 10s during the whole measurement and gathered sound velocity profiles with about 30 minute interval. The first measurement started at 13:26 local time.

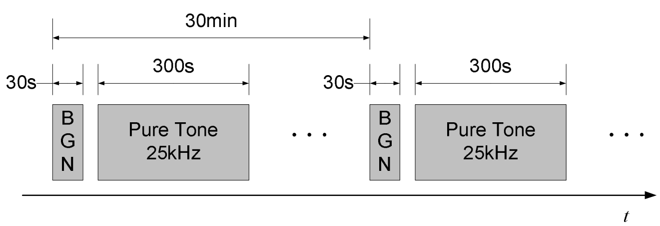

Figure 2. Timeline of the measured data.

III. Experimental Results

A. Environmental Data

Fig. 3(a) shows measured sound velocity profiles. In the early afternoon sound refracts upward direction (the right 4 lines) whereas refraction becomes smaller in the late afternoon (the left 2 lines). From the data we can say that the ray bending is not severe in the measurement situation. Fig. 3(b) shows measured wind speed. It varies from 4 to 10m/s and the average value is about 7m/s. The highest value is measured at around 13:30 and the lowest one is at around 15:40. Fig. 3(c) shows the estimated distance between the transmitter and receiver. Because the surface vessels were moored, the distance is continuously changing. The main causes of the change were tidal current and wind. The rms error of the GPS might also affect the results. Fig. 3(d) shows the background noise. The power spectral density was obtained with the spectral resolution of 100Hz. Higher noise levels are observed between 14:26 and 15:26 (the fourth and fifth measurements).

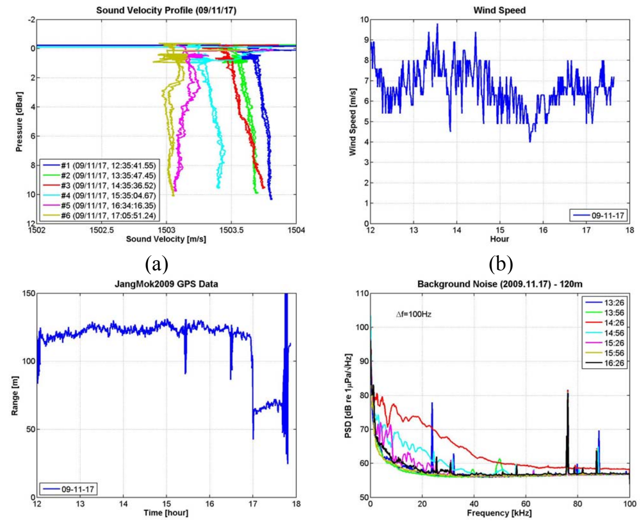

(a) (b) (c) (d)

Figure 3. Measured environmental data.
(a) sound velocity profiles (b) wind speed (c) distance between transmitter and receiver (d) background noise

B. Doppler Spectrum and Spaced-time Correlation

Fig. 4(a) shows power spectral densities (PSDs) of the baseband data. Their resolution is 0.1Hz. The results show that the Doppler effect is very small. The transmitting power during the first measurement was 10dB higher than the others. Note that the blue line is also about 10dB higher than the others. Fig. 4(b) depicts the PSDs of normalized baseband data. The normalization process is applied for the baseband data to have unit power. The third measurement data has the broadest spectrum.

Spaced-time correlation is depicted in Fig. 5. The correlation times are different for each measurement. That means channel condition is changing continuously.

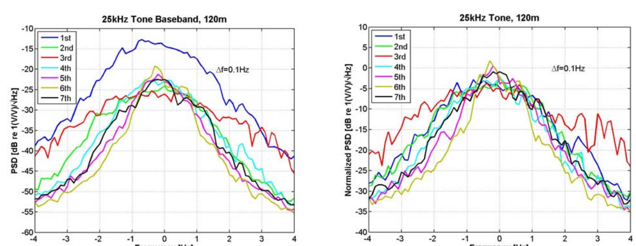

(a) (b)

Figure 4. Doppler spectrum (0.1Hz resolution)
(a) before normalization (b) after normalization

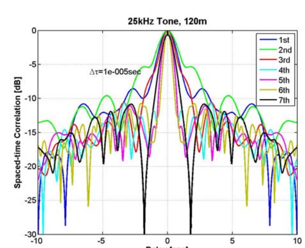

Figure 5. Spaced-time correlation

C. PDFs and CDFs

The bandwidth of the transmitting signal is narrow so that the receiver cannot resolve each multi-path signals. The received signals represent the sum of complex amplitudes for all the multi-paths. Figs. 6(a) and 6(b) show PDFs and CDFs of magnitude from each data set. Theoretically the PDF of magnitude is known to be a Rician function when there is a line of sight path with scattered signal [8]. The graphs of Fig. 6(a) look similar to Rician distribution. The shapes do not coincide each other and this means the channel conditions are different for each measurements. Figs. 6(c) and 6(d) are PDFs and CDFs of phase. For random media and random transducer positions phase is also random. In that case PDF must have uniform distribution and CDF is linear theoretically. Although there are ripples in Fig. 6(c) we can say that the PDFs have almost constant value, $1/2\pi$.

For underwater acoustic communication using coherent modulation techniques not only phase but also phase change is a critical parameter. We also estimate PDFs and CDFs of phase change rate as shown in Figs. 6(e) and 6(f). The shapes are similar to Gaussian distribution with zero mean. The first measurement (blue line) has the smallest variance. Reminding that the transmitting power is 10dB higher than the others, one can interpret that low SNR induces high randomness so that phase change rate can have higher values.

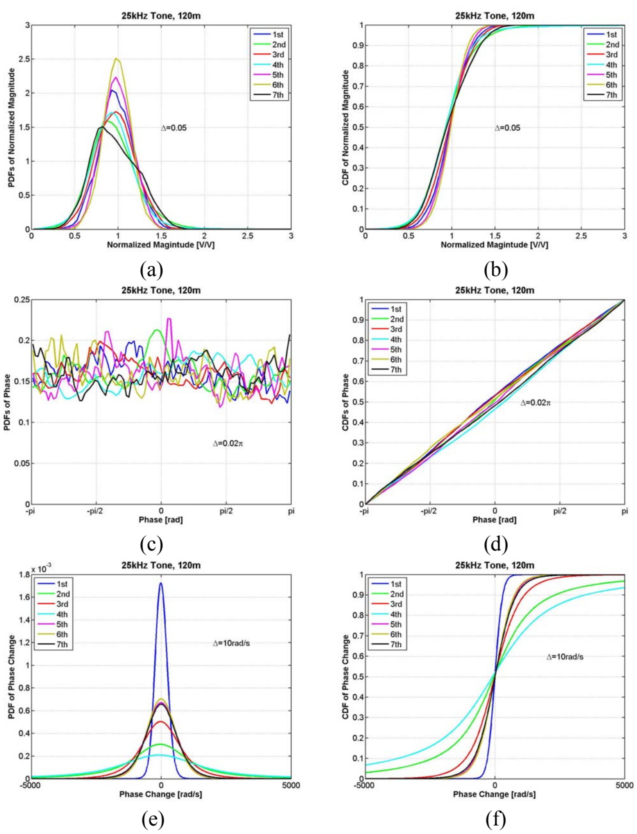

Figure 6. PDFs and CDFs
(a) PDFs of magnitude (b) CDFs of magnitude (c) PDFs of phase (d) CDFs of phase (e) PDFs of phase change rate (f) CDFs of phase change rate

D. Estimation of Parameters by Curve Fitting

In order to analyze quantitatively the change of the distribution statistical parameters are estimated by curve fitting. We assume Rician and Gaussian distributions for magnitude and phase change rate respectively as following equations.

$$p_R(x;s,\sigma)=\frac{x}{\sigma^2}e^{-\left(x^2+s^2\right)/2\sigma^2}I_0\left(\frac{xs}{\sigma^2}\right) \quad (1)$$

$$p_G(x;\mu,\sigma)=\frac{1}{\sqrt{2\pi}\sigma}e^{-(x-\mu)^2/2\sigma^2} \quad (2)$$

In Eq. (1) I_0 stands for the zero-th order modified Bessel function. Note that Rayleigh distribution is the special case of Ricain distribution (when s=0). Fig. 7(a) shows estimated values of s in Eq. (1). The parameter s is placed between 0.8 and 1.0, which means the magnitude does not satisfy the Rayleigh distribution any more. That is the result we have for the mid-range condition in previous experiments [7]. Estimated parameter σ is shown in Fig. 7(b). As s becomes larger σ becomes smaller. The smallest and largest values of σ are obtained in the sixth and seventh cases. Although the parameters are changing the difference between the maximal and minimal value is not large.

Fig. 7(c) shows the error between the measured and estimated PDFs. The error is calculated using the Eq. (3).

Whereas the sixth measurement result fits well to Rician distribution the seventh does not. Fig. 8 compares the measured and fitted curves for the two cases. In Fig. 8(a) two

$$error=\sqrt{\sum_i\left(p_{measure}(i\Delta)-p_R(i\Delta;s,\sigma)\right)^2} \quad (3)$$

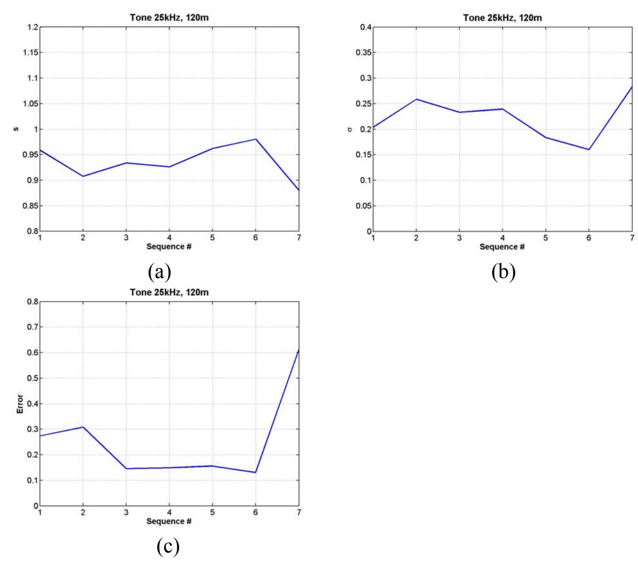

Figure 7. Parameter estimation and its error
(a) s (b) σ (c) error

curves match well and the measured data can be said to have a Rician distribution. In Fig. 8(b) two curves do not match well and it is hard to say the data have the Rician distribution property. From this point we can say that the distributions are different at different time although the frequency and distance have same values.

Fig. 9(a) depicts the estimated mean value μ. The value μ is proportional to the total change of phase (final phase – initial phase). It is also related to Doppler in the signal. If there is no Doppler μ must be zero. μ of fourth data set is about -80 but it is still small value compared to the standard deviation. Fig. 9(b) shows estimated σ, the square root of variance. The first data set has the smallest variance and the fourth one has the largest.

Fig. 10 compares the measured and fitted curves for the two cases. Although the distribution of the fourth case is slightly different from Gaussian distribution, it is evident that the propagation channel condition varies continuously.

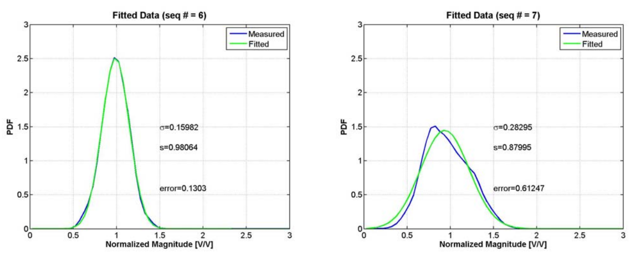

(a) (b)

Figure 8. Curve fitting results for distribution of magnitude
(a) the sixth measurement (b) the seventh measurement

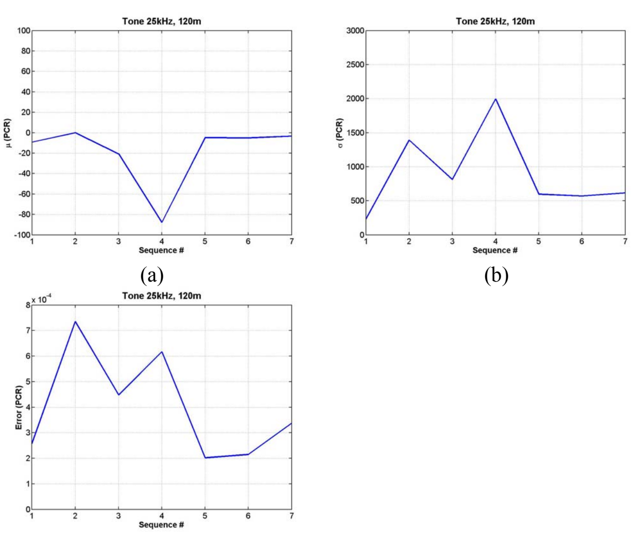

(a) (b) (c)

Figure 9. Parameter estimation and its error
(a) μ (b) σ (c) error

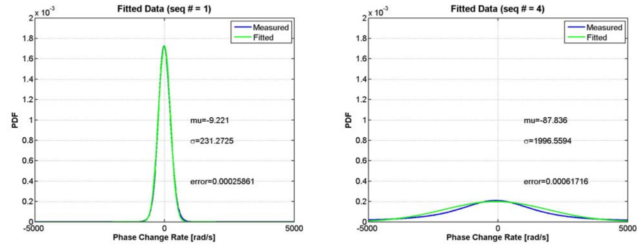

(a) (b)

Figure 10. Curve fitting results for distribution of phase change rate
(a) the first measurement (b) the fourth measurement

IV. CONCLUSION

Pure tone signals are measured in shallow water near the southern coast of Korea. Data are gathered for 300s with an interval of 30 minutes for a long time. PDFs of magnitude, phase, and phase change rate are obtained for each data set. The PDFs of magnitude and phase change rate are similar to Rician and Gaussian distributions respectively. Their statistical parameters are estimated assuming the same distributions. The results show that all the properties are continuously changing with a certain amount of values.

ACKNOWLEDGMENT

The authors would like to thank our colleagues, G.-S. Kim, D.-H. Lee, and Y.-M. Choo at MOERI/KORDI, who have helped gather measurement data at Jinhae Bay.

REFERENCES

[1] R. J. Urick, *Principles of Underwater Sound*, 3rd Ed., McGraw-Hill: New York, 1983, p. 282.
[2] X. Geng and A. Zielinski, "An eigenpath underwatr acoustic communication channel model," *Oceans 1995*, pp. 1189-1196, 1995.
[3] T. C. Yang, "Temporal fluctuations of broadband channel impulse functions and underwater acoustic communications at 2-5kHz," *Oceans 2002*, pp. 2395-2400, 2002.
[4] B. Borowski, "Characterization of a very shallow water acoustic communication channel," Oceans 2009 Biloxi.
[5] S.-M. Kim, S.-H. Byun, and Y.-K. Lim, "Experimental analysis of statistical characteristics of a very shallow underwater acoustic channel," J. Acoust. Soc. Am., Vol. 123, No. 5, Pt. 2, p. 3902, 2008.
[6] S.-H. Byun, S.-M. Kim, Y.-K. Lim, and W. Seong, "Measurement of angular power profile at an array receiver in a shallow underwater acoustic channel," J. Acoust. Soc. Am., Vol. 123, No. 5, Pt. 2, p. 3903, 2008.
[7] S.-M. Kim, S.-H. Byun, S.-G. Kim, and Y.-K. Lim, "Experimental analysis of statistical properties of underwater channel in a very shallow water using narrow and broadband signals," *Oceans* 2009 Biloxi.
[8] M. Patzold, *Mobile Fading Channels*, John Wiley & Sons, 2002.